Article:
Konijnenberg, A, Ranica, S, Narkiewicz, J et al. (4 more authors) (2016) Opposite Structural Effects of Epigallocatechin-3-gallate and Dopamine Binding to α-Synuclein. Analytical Chemistry, 88 (17). pp. 8468-8475. ISSN 0003-2700

https://doi.org/10.1021/acs.analchem.6b00731

Supporting Information

for

Opposite structural effects of epigallocatechin-3-gallate and dopamine binding to α-synuclein

Albert Konijnenberg[1], Simona Ranica[2], Joanna Narkiewicz[3], Giuseppe Legname[3], Rita Grandori[2], Frank Sobott[1,4,5,*], and Antonino Natalello[2,6,*]

1) Biomolecular & Analytical Mass Spectrometry, University of Antwerp, Groenenborgerlaan 171, 2020 Antwerp, Belgium;

2) Department of Biotechnology and Biosciences, University of Milano-Bicocca, Piazza della Scienza 2, 20126 Milan, Italy;

3) Department of Neuroscience, Scuola Internazionale Superiore di Studi Avanzati (SISSA) and ELETTRA - Sincrotrone Trieste S.C.p.A, 34136 Trieste, Italy;

4) Astbury Centre for Structural Molecular Biology, University of Leeds, Leeds, LS2 9JT, UK;

5) School of Molecular and Cellular Biology, University of Leeds, Leeds, LS2 9JT, UK;

6) Consorzio Nazionale Interuniversitario per le Scienze Fisiche della Materia (CNISM), UdR of Milano-Bicocca, and Milan Center of Neuroscience (NeuroMI), 20126 Milan, Italy.

*Corresponding Authors

Frank Sobott, E-mail: frank.sobott@uantwerpen.be

Antonino Natalello, E-mail: antonino.natalello@unimib.it

CONTENTS

Supporting information for the EXPERIMENTAL SECTION (materials and sample preparation and nano-ESI-MS analysis), 18 supporting figures and 8 supplementary references.

EXPERIMENTAL SECTION

Materials and sample preparation. Ammonium acetate, ammonium hydroxide, dopamine (DA; calculated monoisotopic mass 153.08 Da), epigallocatechin-3-gallate (EGCG; calculated monoisotopic mass 458.08 Da), cytochrome c (CytC) from horse heart, and formic acid were purchased from Sigma Aldrich (St. Louis, MO).

Wild-type human α-synuclein (AS; average mass 14460.1 Da) was expressed in recombinant form and purified as previously described[1]. After sample desalting against 100 mM ammonium acetate pH 7.4 on PD-10 columns (Amersham Biosciences, Amersham UK) to promote sodium displacement, aliquots were lyophilized and stored at -80°C.

Nano-ESI mass spectrometry. The stock solution of EGCG (1 mM) was prepared in 10 mM ammonium acetate pH 7.4. The stock solution of DA (100 mM) was prepared in 10 mM ammonium acetate pH 5 and then diluted at least 20-fold in 10 mM ammonium acetate pH 7.4 immediately before the experiments. The final pH of the solutions was checked by the Crison Basic20 pH meter (Crison Instruments, Barcelona, Spain). Titrations by EGCG were performed up to 200 µM ligand concentration, due to poor spectral quality at higher EGCG concentrations.

MS spectra were collected upon 10-min incubation of the protein-ligand mixtures at room temperature.

Nano-ESI-MS spectra were generally collected in positive-ion mode, using a hybrid quadrupole-time-of-flight mass spectrometer (QSTAR-Elite, Biosystems, Foster City, CA) equipped with a nano-ESI sample source. In control experiments, mass spectra were also measured in negative-ion mode[2]. Samples were infused by metal-coated borosilicate capillaries (Proxeon, Odense, Denmark) with medium-length emitter tip of 1-µm internal diameter. The instrumental parameters were optimized as previously described[2] and set at the following values: +1150/+1200 V ion-spray voltage, +80 V declustering potential, 20 PSI curtain-gas pressure, and room-temperature for the instrument interface. The spectra were averaged over 3-5 min.

Deconvoluted spectra were obtained using the Bayesian protein reconstruct tool of BioAnalyst™ extension of Analyst QS 2.0 software (Applied Biosystems, Foster City, CA).

The relative intensity of the protein-ligand complex ions (PL) with charge state 8+ or 15+ was calculated as follows:

$$I_{PL} = \frac{\sum_{i=1}^{N} I(PL_i^{n+})}{\sum_{i=0}^{N} I(PL_i^{n+})} 100$$

where i (from 0 to N) is the number of ligand molecules L bound to the AS monomer P; I is the intensity of the bound and unbound protein ions with charge n+.

The theoretical distribution of protein-ligand complexes with different stoichiometries was calculated considering three or four independent and identical binding sites[3,4]. The theoretical distributions were compared with the experimental distribution obtained from the sample with 20 µM AS and 0.5 mM DA or 6 mM DA at the same value of *ν*, representing the average number of bound ligand molecules per protein molecule:

$$\nu = \frac{[L]_{bound}}{[P]_{total}}$$

This value can be calculated from the mass spectra according to the following equation:

$$\nu = \frac{[L]_{bound}}{[P]_{total}} = \frac{\sum_{i=0}^{N} i \sum_{n+} I(PL_i^{n+})}{\sum_{i=0}^{N} \sum_{n+} I(PL_i^{n+})}$$

where the summation is extended over all the n+ charge states detected in the mass spectra.

SUPPORTING FIGURES

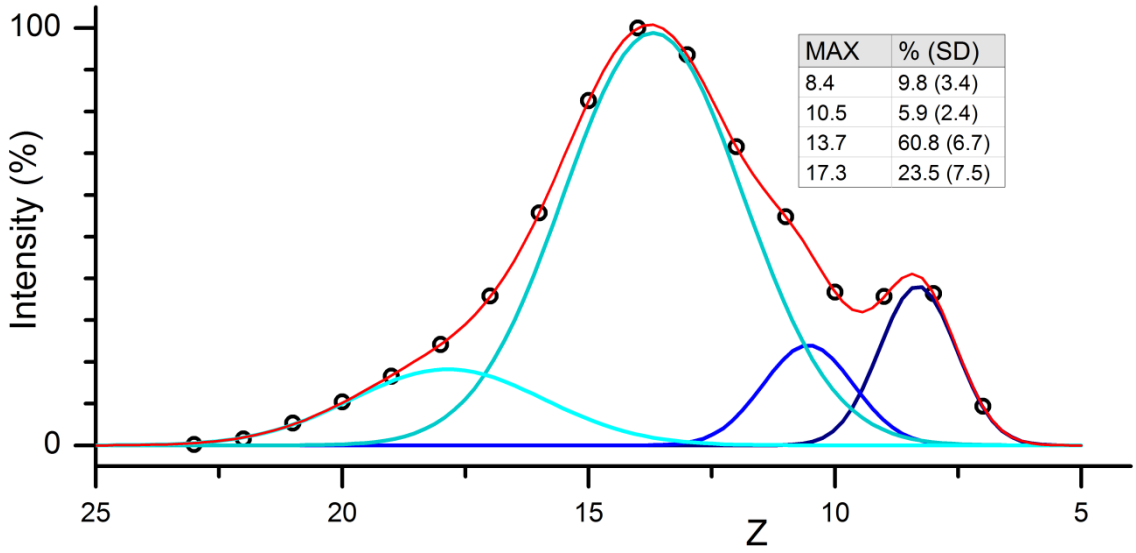

Figure S-1. Gaussian fitting of charge state distribution.
Deconvolution of a representative nano-ESI-MS spectrum of 20 μM AS. The values reported in the inset refer to the area of each component (MAX, main charge state; SD, standard deviation) and were obtained by averaging the deconvolution results of four repeats using independent protein preparations. For this analysis, the data were plot as ion relative intensity versus charge and then fitted by Gaussian functions. The number of components and their initial maxima were taken from Frimpong et al.[5] The parameters were then let free to change to optimize the final fitting. The calculations were performed by the software Origin 8 (Originlab, Northampton, MA, USA).

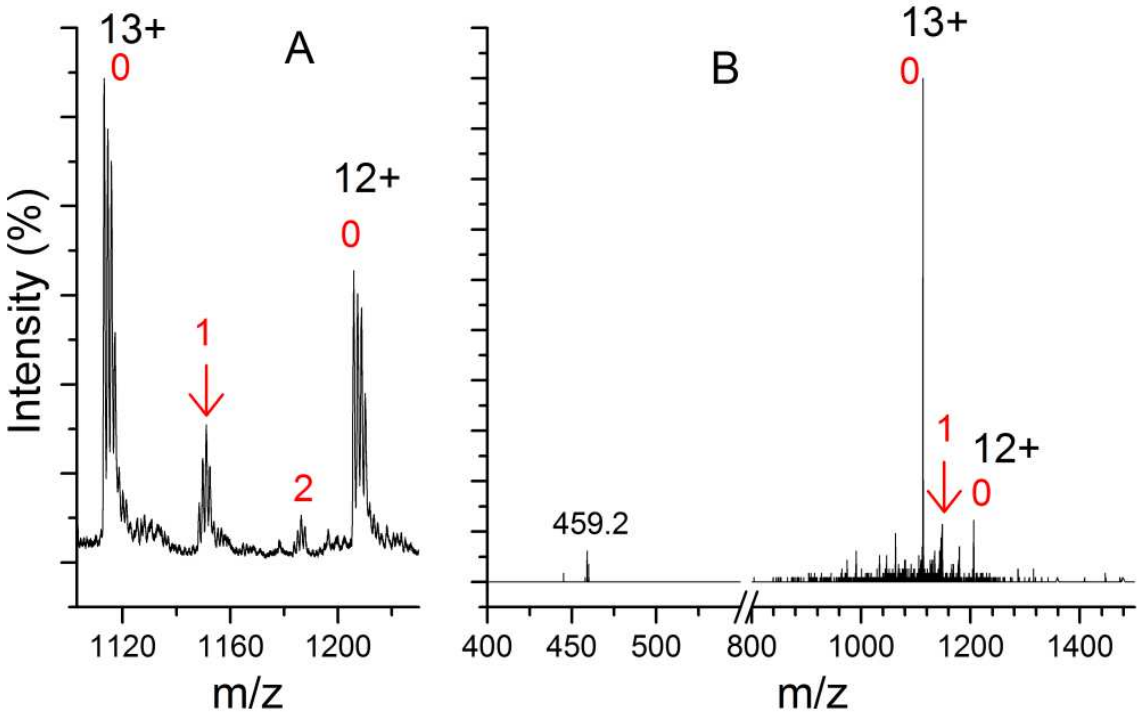

Figure S-2. Dissociation of AS-EGCG complexes in positive-ion mode.
(A) Nano-ESI-MS spectrum of 20 µM AS and 100 µM EGCG in the spectral region of the 13+ AS monomer. (B) MS/MS spectrum of the AS-EGCG complex. The number of EGCG molecules in each complex is indicated in red. Arrows indicate the precursor ion. The applied collision energy was 23 V. The 459.2 m/z peak corresponds to the $[EGCG+H]^+$ ion (see Fig. S-3). Detection of the free ligand with intact mass upon CID is consistent with a non-covalent nature of the complex. Predominance of the 13+ protein ion among the products indicates that EGCG dissociates prevalently as a neutral species. The signals of the 12+ protein and the $[EGCG+H]^+$ ions are due, instead, to dissociation events with departure of protonated ligand from the complex.

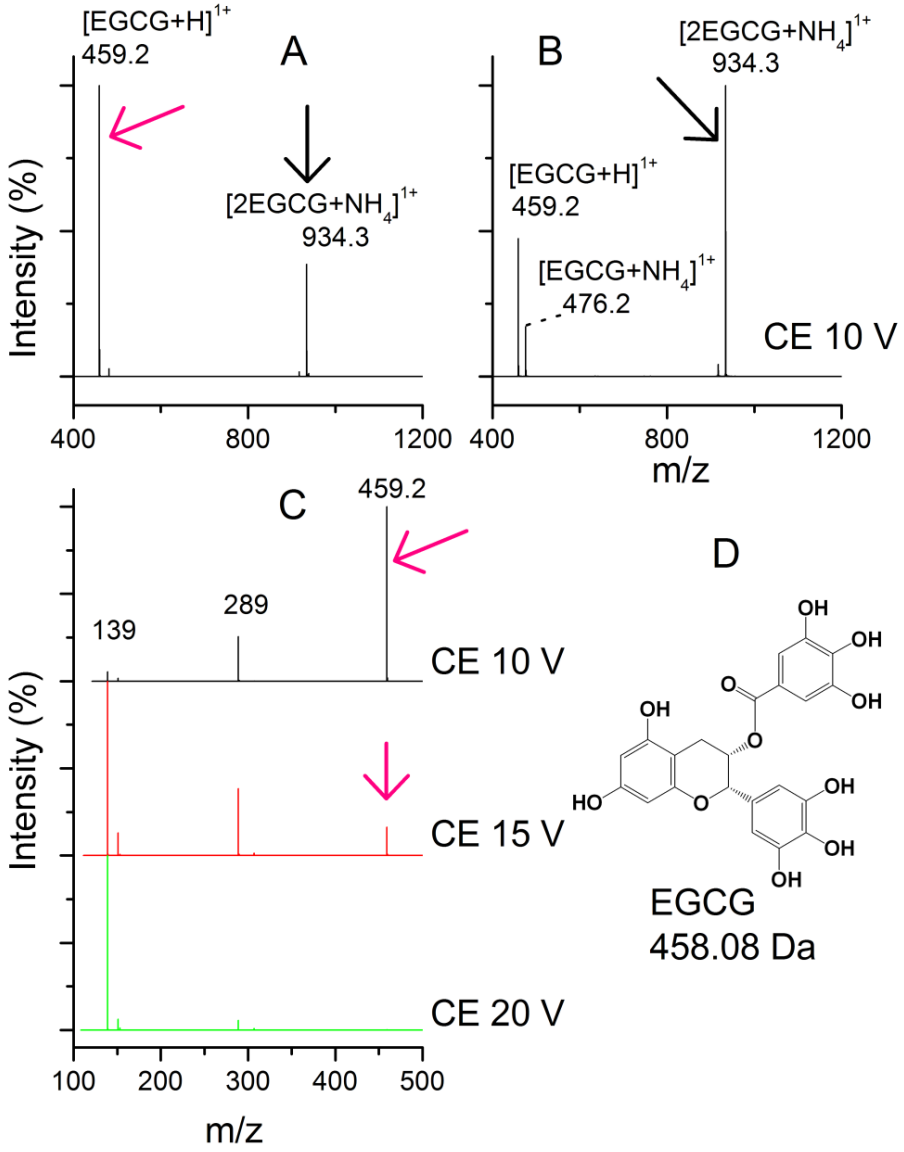

Figure S-3. EGCG fragmentation in positive-ion mode.
(A) Nano-ESI-MS spectrum of 500 µM EGCG. (B) MS/MS spectrum of the 934.3 m/z ion from (A). (C) MS/MS spectra of the 459.2 m/z ion from (A). The characteristic fragment ions of gallocatechin gallates at 289 m/z and 139 m/z are observed[6]. Arrows indicate the precursor ions. The applied collision energy (CE) is also given. (D) Chemical structure and calculated monoisotopic mass of EGCG.

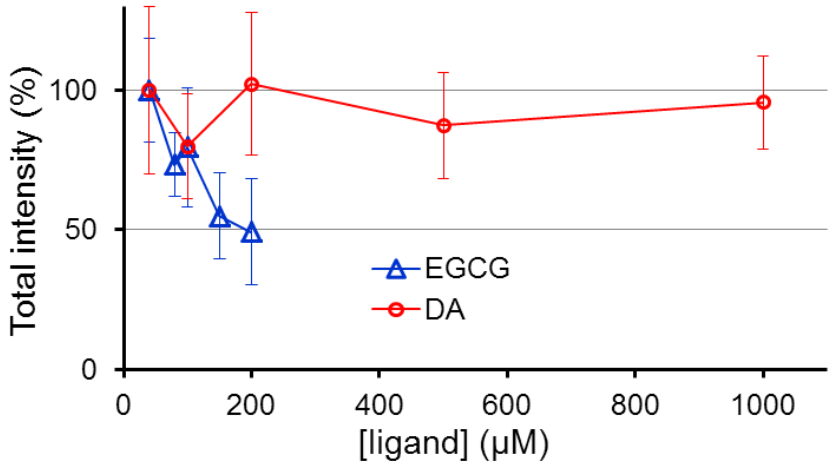

Figure S-4. Total ion intensity as a function of EGCG or DA concentration.
The spectra were collected in positive-ion mode. The intensity in the presence of DA drops to 36% at 6 mM ligand (data not shown), which could also be explained by the high analyte concentration.

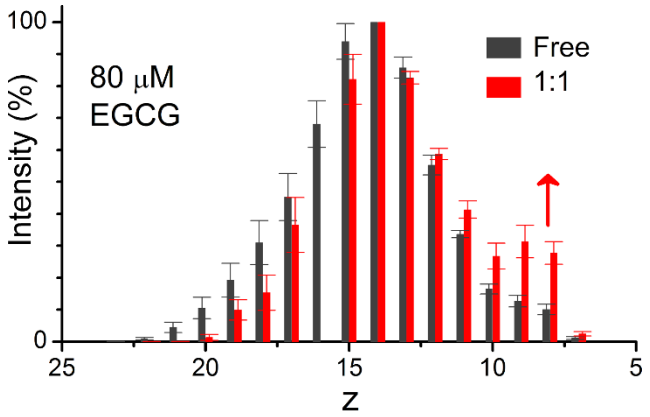

Figure S-5. Charge state distributions of the free and bound AS forms for 20 µM AS in the presence of 80 µM EGCG. The 16+ peak of the AS-EGCG complex was omitted due to overlap with the ammonium adduct of the EGCG dimer. Error bars represent the standard deviation from three independent experiments.

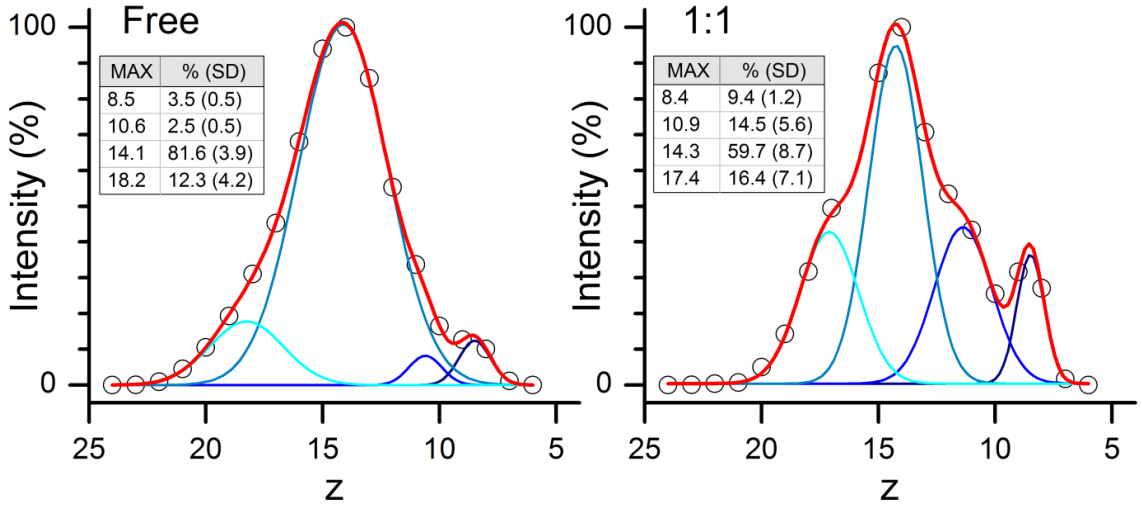

Figure S-6. Gaussian fitting for the free and bound AS forms.
The nano-ESI-MS data obtained in positive-ion mode for 20 µM AS, in the presence of 80 µM EGCG, were plot as ion intensity versus charge and then fitted by Gaussian functions as in Fig. S-1. The 16+ peak of the AS-EGCG complex was omitted due to overlap with the ammonium adduct of the EGCG dimer. The values reported in the inset refer to the area of each component (MAX, main charge state; SD, standard deviation) and were obtained by averaging the deconvolution results from three independent experiments.

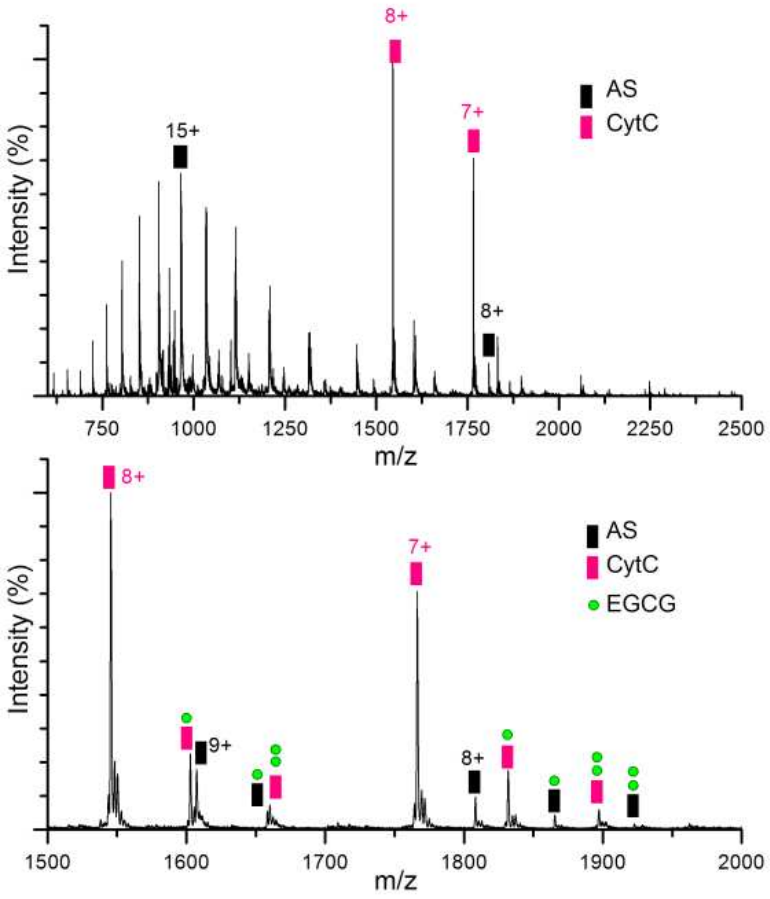

Figure S-7. Nano-ESI-MS spectrum in positive-ion mode of 20 µM AS, 20 µM cytochrome c (CytC), and 100 µM EGCG.
The MS data are reported in the 600-2500 m/z and 1500-2000 m/z spectral regions.
Charge states are indicated in black for AS and pink for CytC, for some selected ion**s.**

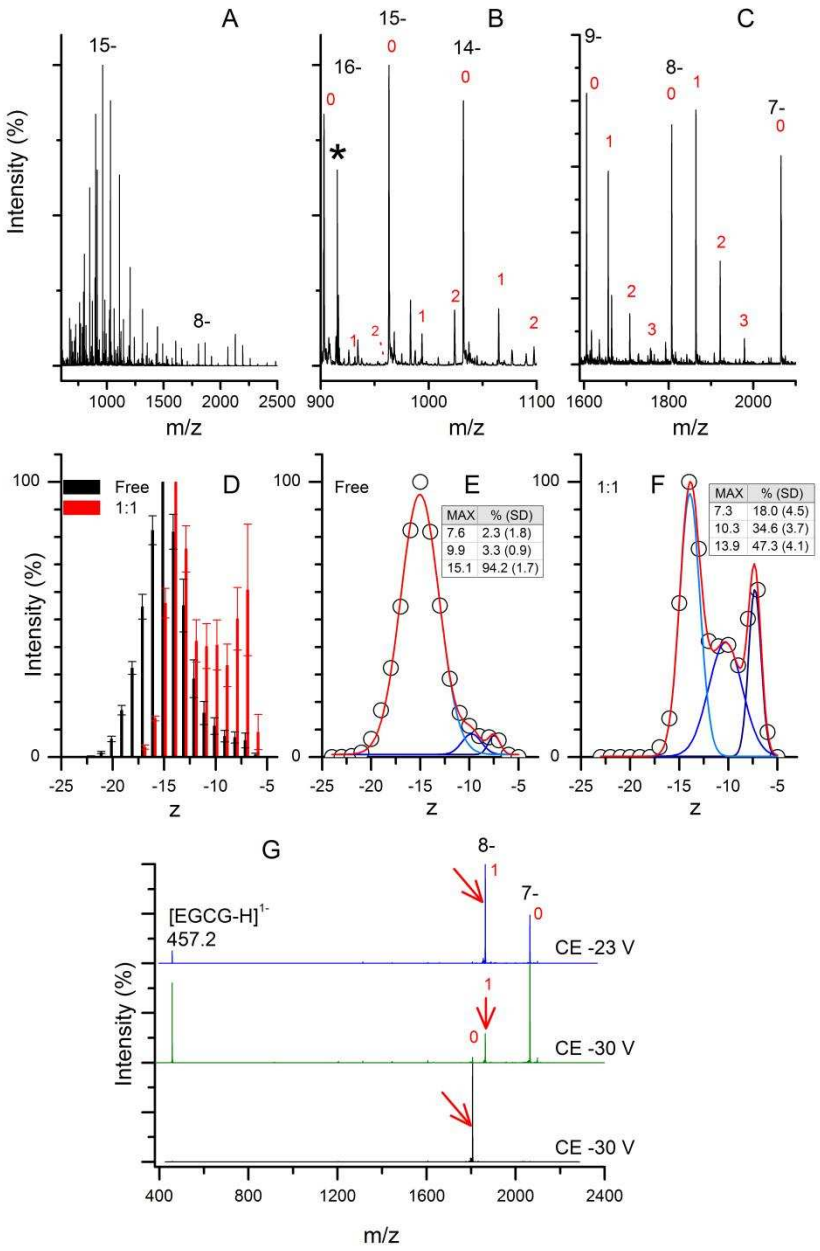

Figure S-8. AS-EGCG complexes in negative-ion mode.
(A-C) Nano-ESI-MS spectra in negative-ion mode of 20 µM AS, in the presence of 150 µM EGCG. The following spectral regions are shown: 600-2500 m/z (A), 900-1100 m/z (B), and 1590-2100 m/z (C). The number of EGCG molecules in each complex is indicated in red, for selected ions. A star indicates the EGCG dimer. (D) CSD of the free and bound AS forms, for 20 µM AS in the presence of 150 µM EGCG. Error bars represent the standard deviation from three independent experiments. (E,F) Gaussian fitting of the data from panel (D). The data were plot as ion intensity versus charge and then fitted by Gaussian functions as in Fig. S-1. The values reported in the inset refer to the area of each component (MAX, main charge state; SD, standard deviation) and were obtained by averaging the deconvolution results from three independent experiments. (G) MS/MS spectra of the 1:1 AS:EGCG complex for the sample containing 20 µM AS, 100 µM EGCG (blue and green) and of AS alone for the sample containing 20 µM AS (black). The arrows indicate the precursor ions. The charge states are indicated only in the upper spectrum. The number of EGCG molecules in each complex is indicated in red. The applied collision energy (CE) is also given.

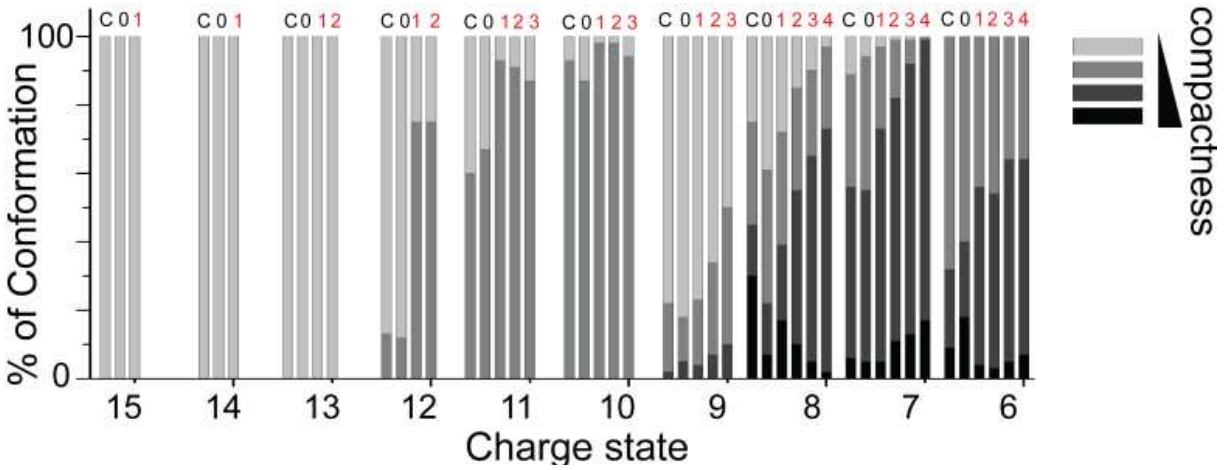

Figure S-9. IM-MS reveals EGCG-induced compaction of low-charge AS monomers. Relative amounts of the different conformations of AS detected for any charge state where EGCG binding was observed, as a function of the number of EGCG molecules bound. C, control sample in the absence of the ligand.

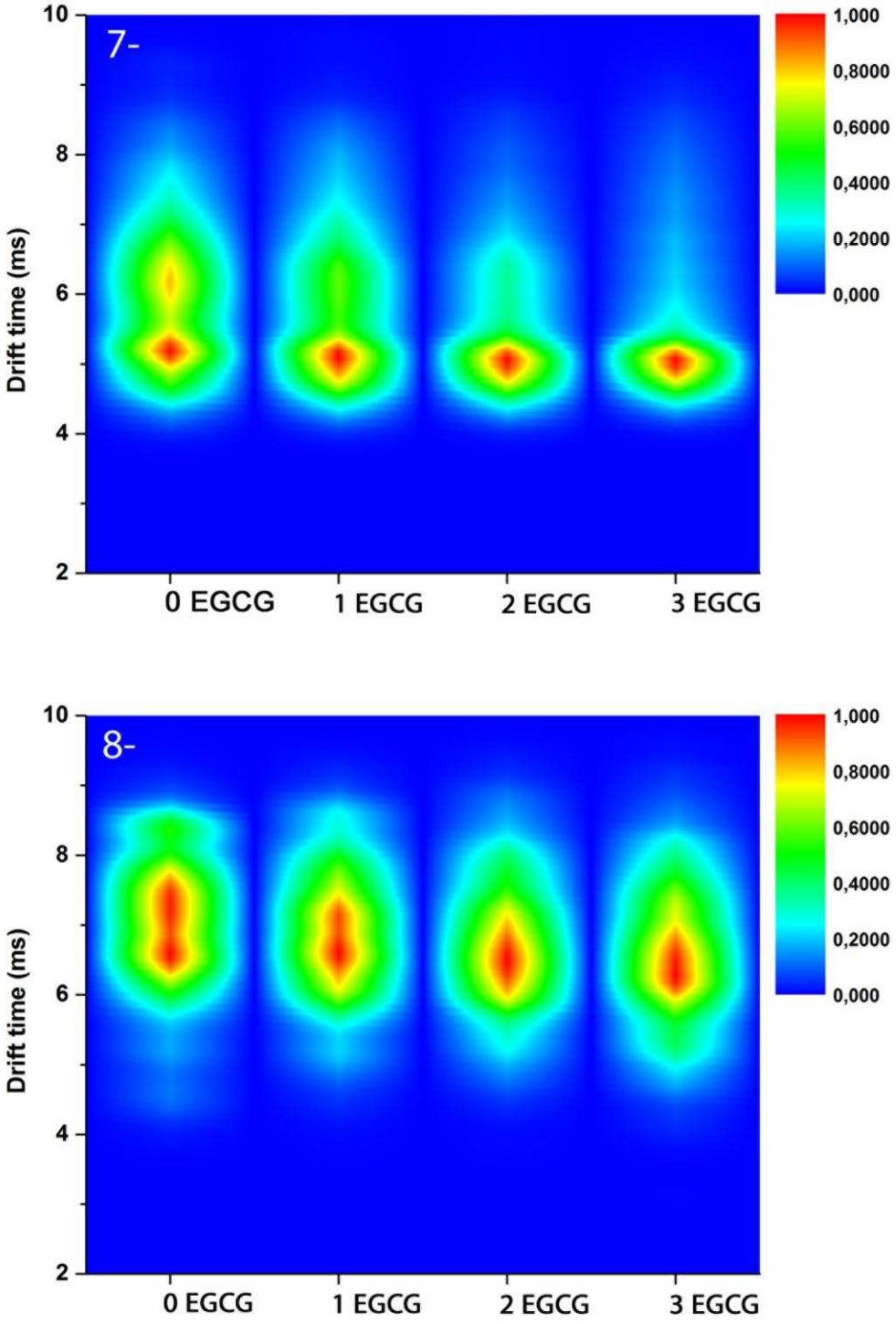

Figure S-10. IM-MS of AS-EGCG complexes in negative ion mode reveals that EGCG-induced compaction is independent of ionization mode. Heat maps of the conformations observed for (top) the 7- and (bottom) the 8- charge state upon binding increasing numbers of EGCG.

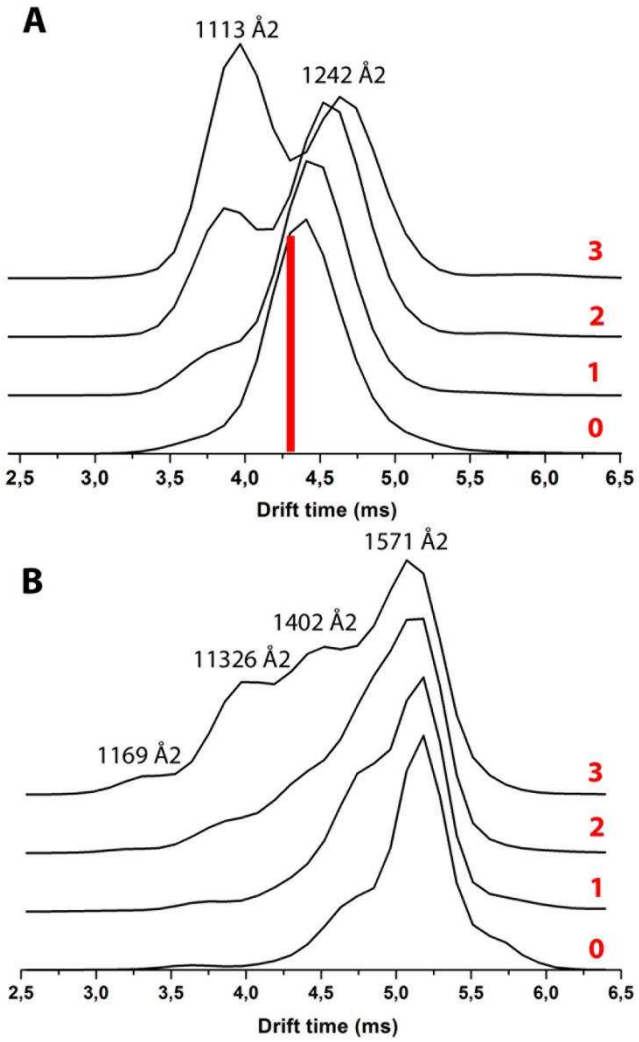

Figure S-11. IM-MS analysis of CytC-EGCG complexes.
EGCG induces conformational compaction for the (A) 6+ and (B) 7+ charge state of native CytC, similar to what is observed with AS. Red line in (A) indicates the theoretical CCS for CytC based on the crystal structure (PDB-ID: 1GIW) and red numbers indicate the number of EGCG molecules bound.

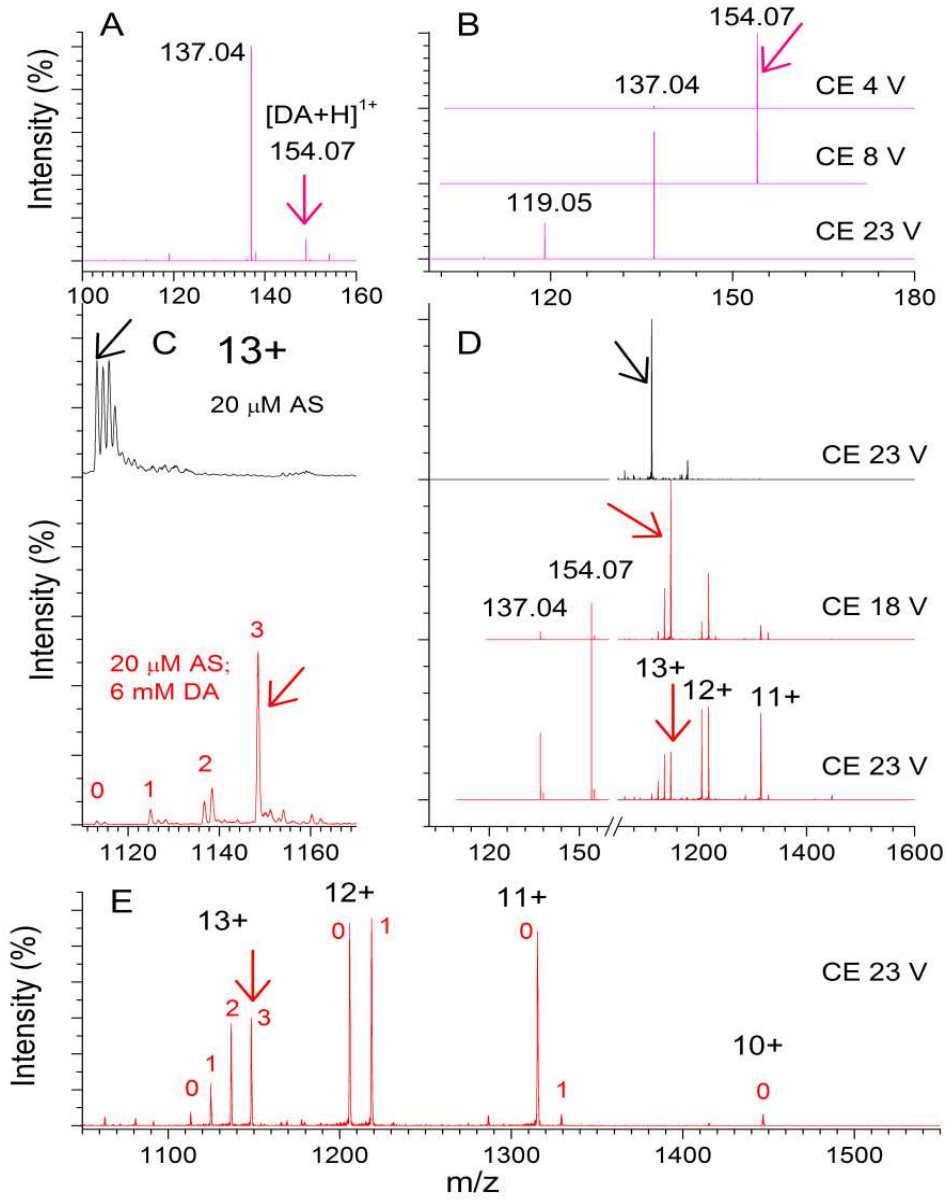

Figure S-12. AS-DA complexes in positive-ion mode.
(A) Nano-ESI-MS spectrum of 100 µM DA. (B) MS/MS spectra of protonated DA. The applied collision energy (CE) is also given. The 137.04 m/z and 119.05 m/z peaks can be assigned, respectively, to the loss of NH_3 and NH_3 + H_2O from protonated DA (154.08 Da)[7,8]. (C) Nano-ESI-MS spectra of 20 µM AS in the absence (black) and in the presence (red) of 6 mM DA in the spectral region of the 13+ AS monomer. The number of DA molecules in the complexes are indicated in red. (D) MS/MS spectra of the 13+ ion of free AS (black) and AS-DA_3 complex (red). Protein product ions are labeled by the charge state, DA product ions are labeled by mass. (E) Enlargement of the protein product ions shown in (D). The number of DA molecules in each complex is indicated in red.
Precursor ions indicated by the arrows.

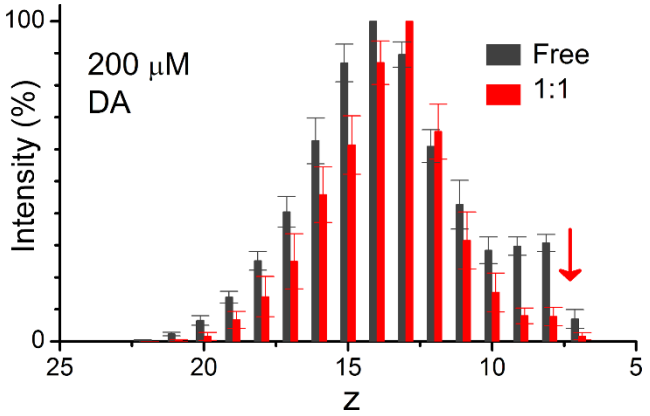

Figure S-13. Charge state distributions of the free and bound AS forms for 20 µM AS in the presence of 200 µM DA. Error bars represent the standard deviation from three independent experiments.

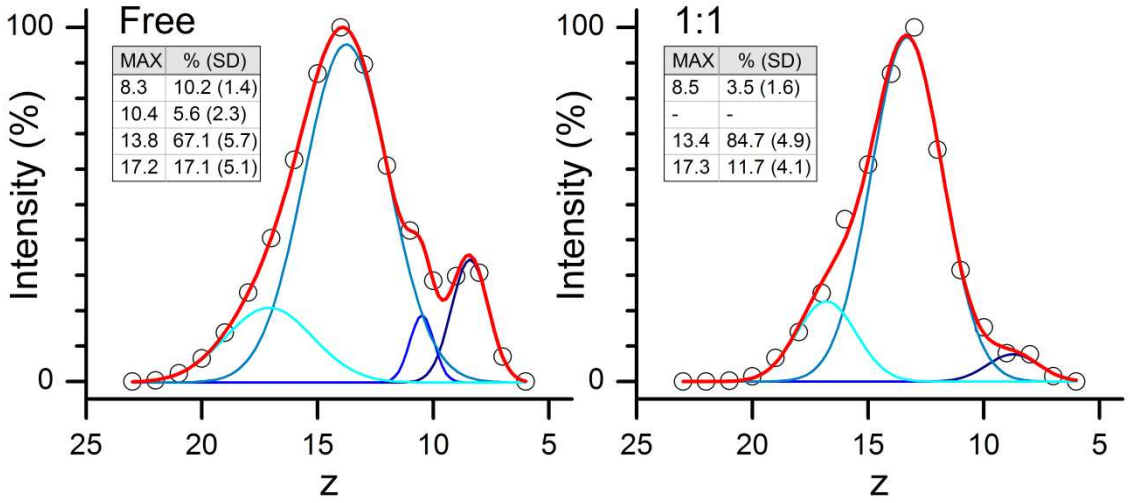

Figure S-14. Gaussian fitting for the free and bound AS forms.
The nano-ESI-MS data obtained in positive-ion mode for 20 µM AS, in the presence of 200 µM DA, were plot as ion relative intensity versus charge and then fitted by Gaussian functions as in Fig. S-1. The values reported in the inset refer to the area of each component (MAX, main charge state; SD, standard deviation) and were obtained by averaging the deconvolution results from three independent experiments.

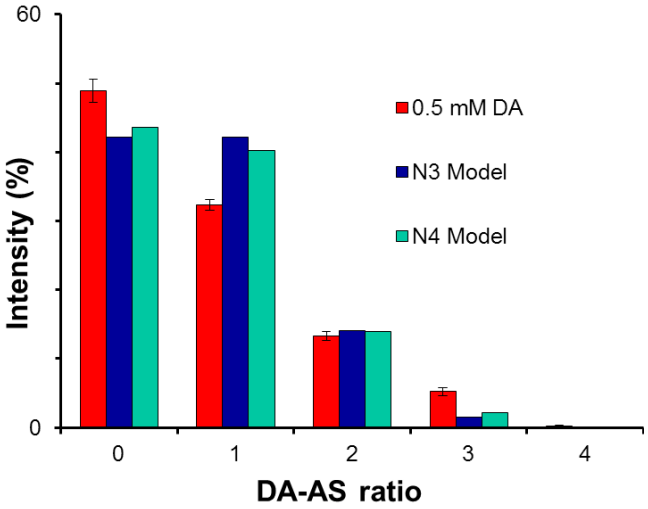

Figure S-15. Species distribution of AS-DA complexes of distinct stoichiometry as derived from the measurements at 20 µM AS and 0.5 mM DA.
The values calculated according to the 1:3 and 1:4 models, assuming identical and independent binding sites, are also reported. Error bars represent the standard deviation from three independent experiments.

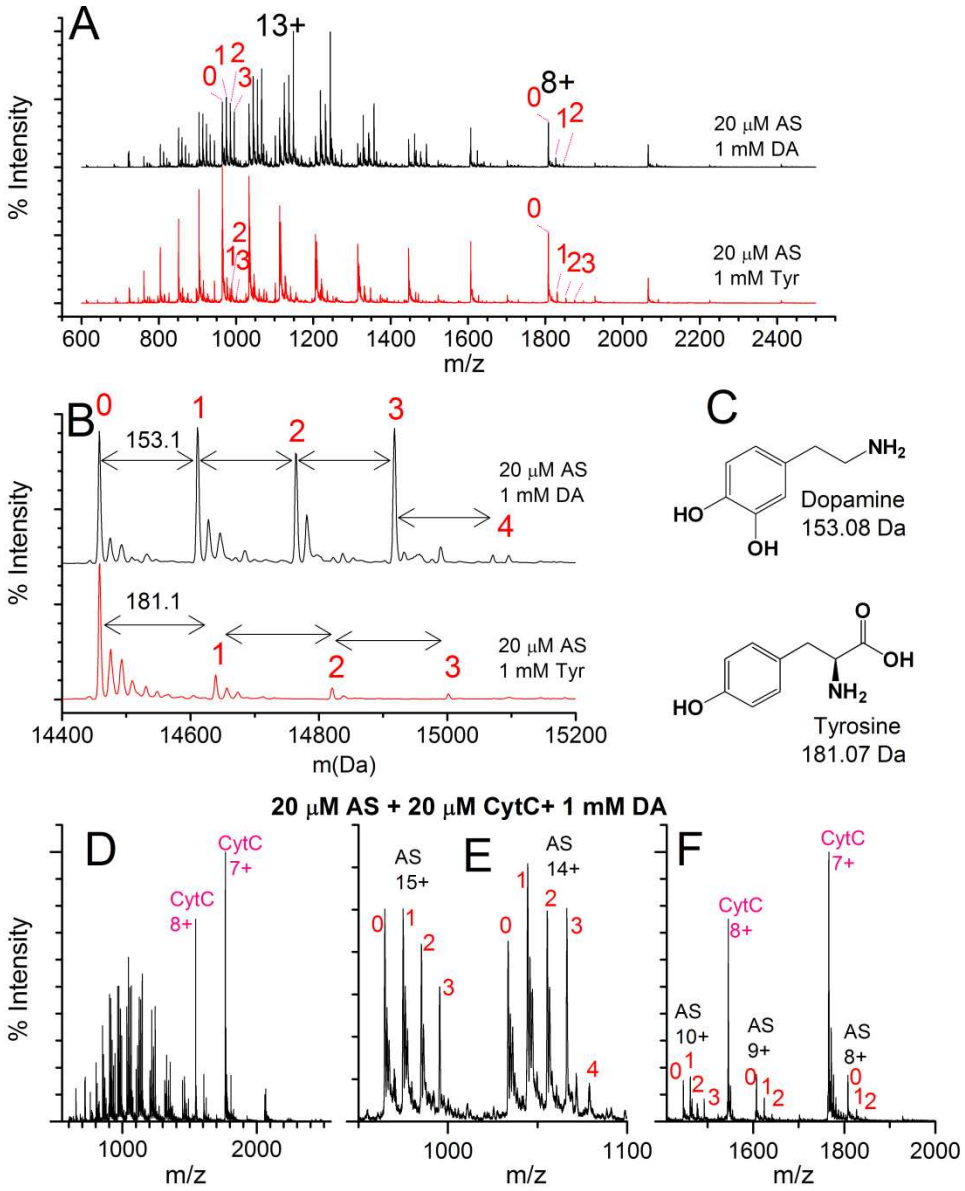

Figure S-16. Selectivity in DA versus tyrosine binding in positive-ion mode.
(A,B) Nano-ESI-MS spectra in positive-ion mode of 20 μM AS in the presence of 1 mM DA or 1 mM tyrosine. (A) Raw spectra, (B) deconvoluted spectra. (C) Chemical structure and calculated monoisotopic mass of DA and tyrosine. (D-F) Nano-ESI-MS spectrum in positive-ion mode of 20 μM AS, 20 μM cytochrome c (CytC), and 1 mM DA for the 600-2500 m/z (D), 950-1100 m/z (E), and 1410-2000 m/z (F) spectral regions. The number of DA molecules for AS monomer is indicated in red, for some selected ions. Charge states are indicated in black for AS and pink for CytC.

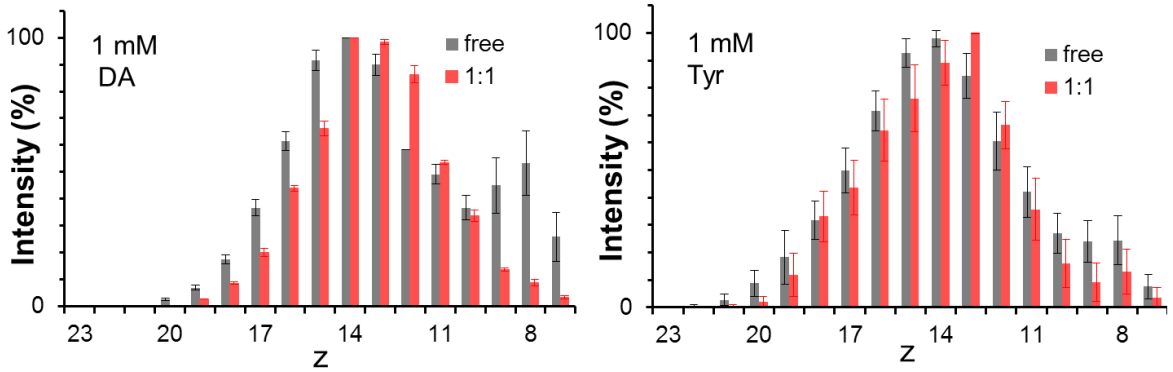

Figure S-17. CSD of the free and bound AS forms for 20 µM AS in the presence of either 1 mM DA or 1 mM tyrosine (Tyr). Error bars represent the standard deviation from three independent experiments.

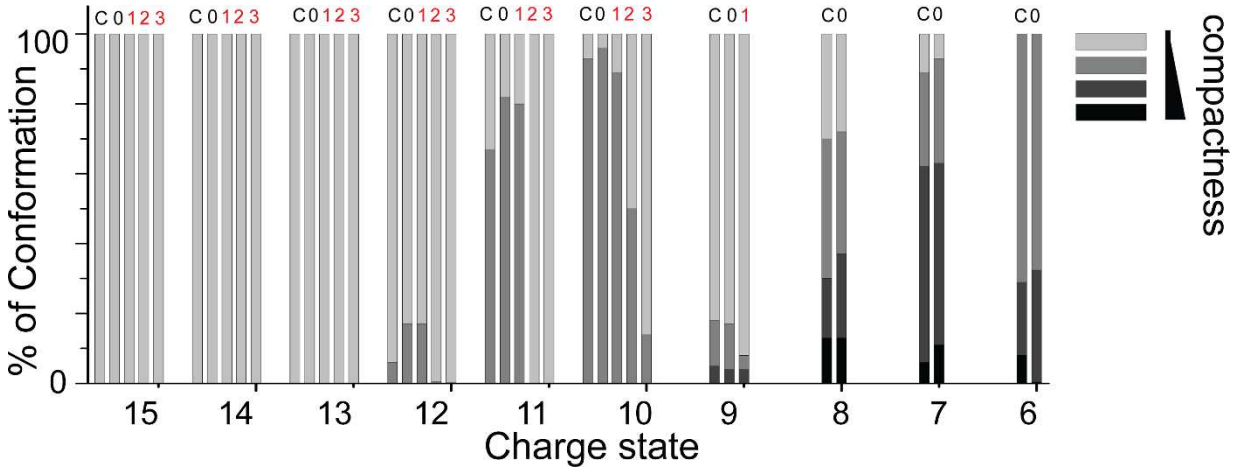

Figure S-18. DA induced elongation of AS monomers observed in the gas phase. Relative amounts of the different conformations of AS detected for any charge state where DA binding was observed, as a function of the number of DA molecules bound. C, control sample in the absence of the ligand.

SUPPLEMENTARY REFERENCES

(1) Latawiec, D.; Herrera, F.; Bek, A.; Losasso, V.; Candotti, M.; Benetti, F.; Carlino, E.; Kranjc, A.; Lazzarino, M.; Gustincich, S.; Carloni, P.; Legname, G. PLoS ONE **2010**, 5(2): e9234.
(2) Natalello, A.; Benetti, F.; Doglia, S. M.; Legname, G.; Grandori, R. Proteins **2011**, 79, 611-621.
(3) Tinoco I, Jr.; Sauer, K.; Wang, J. C. Physical Chemistry: Principles and Applications in Biological Sciences; Prentice Hall: New Jersey, 1978.
(4) Sun, J. X.; Kitova, E. N.; Wang, W. J.; Klassen, J. S. Anal. Chem. **2006**, 78, 3010-3018.
(5) Frimpong, A. K.; Abzatimov, R. R.; Uversky, V. N.; Kaltashov, I. A. Proteins **2010**, 78, 714-722.
(6) Zeeb, D. J.; Nelson, B. C.; Albert, K.; Dalluge, J. J. Anal. Chem. **2000**, 72, 5020-5026.
(7) Bergquist, J.; Silberring, J. Rapid Communications in Mass Spectrometry **1998**, 12, 683-688.
(8) Liljegren, G.; Dahlin, A.; Zettersten, C.; Bergquist, J.; Nyholm, L. Lab Chip. **2005**, 5, 1008-1016.